J Mater Sci (2012) 47:746–753
DOI 10.1007/s10853-011-5850-8

Hydrothermal synthesis of quasi-monodisperse AWO_4 (A = Ca, Sr, and Ba) microspheres

Hongli Pan · Mirabbos Hojamberdiev · Gangqiang Zhu

Received: 9 May 2011 / Accepted: 3 August 2011 / Published online: 13 August 2011

Abstract In this study, quasi-monodisperse AWO_4 (A = Ca, Sr, and Ba) microspheres were fabricated by a facile hydrothermal route at 180 °C for 8 h in the presence of citric acid. The as-synthesized AWO_4 powders were characterized by X-ray powder diffraction (XRD), scanning electron microscopy, transmission electron microscopy and photoluminescence spectroscopy. The XRD results revealed that the hydrothermally formed AWO_4 powders presented a scheelite-type tetragonal structure, and the formation of a secondary phase was not observed. The SEM and TEM observations demonstrated that the AWO_4 powders with uniform sphere-like morphologies could be hydrothermally obtained at 180 °C for 8 h without the use of surfactants. The growth process of quasi-monodisperse $BaWO_4$ microspheres, as a representative of AWO_4, was investigated as a function of hydrothermal processing time, and a possible formation mechanism was proposed. The room temperature photoluminescence properties of AWO_4 powders were studied using an excitation wavelength of 350 nm. The positions of the PL emission peaks were not considerably altered, implying that the energy band gap relating to the blue emission was not much affected by the variation in chemical composition of AWO_4 (A = Ca, Sr, and Ba) microspheres. The obtained quasi-monodisperse AWO_4 microspheres will be potential candidates for a broad range of technological applications, as phosphors, luminescent materials, photocatalysts, etc.

H. Pan (✉)
Department of Physics, Shaanxi University of Technology, Hanzhong 723001, Shaanxi, People's Republic of China
e-mail: honglipan2010@163.com

M. Hojamberdiev
Shaanxi Key Laboratory of Nanomaterials and Nanotechnology, Xi'an University of Architecture and Technology, Xi'an 710055, Shaanxi, People's Republic of China

G. Zhu
School of Physics and Information Technology, Shaanxi Normal University, Xi'an 710062, Shaanxi, People's Republic of China

Introduction

Recent researches have shown that the physical and chemical properties of inorganic materials can be tailored through the modification of their sizes, morphologies, crystallographic orientations, shapes, particle size distributions, and geometries [1–3]. Systematically controlling the formation of micro- and nanocrystals is beneficial for various applications, such as optics, electronics, catalysis, medicine, etc. [4, 5]. Thus, a variety of synthesis processes have been actively developed to manipulate the sizes, morphologies, and dimensions of micro- and nanocrystals in the past two decades [6, 7].

The alkaline earth metal orthotungstates, AWO_4 (A = Ca, Sr, and Ba), are the members of an important inorganic materials family with a distinctive scheelite-type structure and interesting properties, such as excitonic luminescence, thermoluminescence and stimulated Raman scattering behavior [8–11]. In general, these compounds crystallize in an $I4_1/a$ space group with four molecules in each crystallographic cell at ambient atmosphere. The divalent A^{2+} and hexavalent W^{6+} atoms coordinate with eight and four O atoms, respectively, and both of the above sites form an S_4 site symmetry [12]. Hence, they are considered to be potential host materials for a broad range of technological applications, as phosphors, gas sensors, all-solid-state lasers, optical fibers, and the components of electrochromic devices, luminescence, amplifiers, catalysis, microwave systems, and the next generation of scintillation detectors [13–17].

As of now, a number of synthesis methods, including solid state reaction [14], electrochemical [13, 18], microemulsion [19, 20], reverse-micelle [21], hydrothermal [22–24], molten salt [25], sonochemical [26], biomembrane template [27], microwave-hydrothermal [28], and polymer template [29], have been employed to manipulate the shapes and sizes of AWO_4 (A = Ca, Sr, and Ba) micro- and nanostructures. Among these methods, the hydrothermal synthesis is a promising synthetic route that can be well-controlled through an appropriate choice of reaction parameters, such as temperature, time, pH, mineralizer, and surfactant. Moreover, low reaction temperature, mild reaction conditions, size-selective growth, controllable morphology, phase purity, smaller particle size, and narrow particle size distribution are the advantages of the hydrothermal synthesis method.

Recently, considerable efforts have been made to synthesize AWO_4 (A = Ca, Sr and Ba) micro- and nanostructures under hydrothermal conditions at low temperatures. For instance, Su et al. [30] and Chen et al. [31] have fabricated $CaWO_4$ nanocrystallites through the hydrothermal method using citric acid and ethylene glycol as a capping agent and a solvent, respectively. With a particle size reduction, $CaWO_4$ nanocrystallites showed a systematic lattice expansion, lattice vibrational variations and a shift of electronic absorption bands. $CaWO_4$ nanorods with mean lengths of 0.6–1 μm were synthesized by a microemulsion-mediated hydrothermal process using cetyltrimethylammonium bromide (CTAB) [32]. The water/CTAB ratio played a dominant role in the formation of nanorods. Octahedron-, olive-, flake-, and whisker-like $BaWO_4$ crystals were synthesized by the hydrothermal process in the presence of different surfactants [33, 34]. Octahedron-shaped $SrWO_4$ microcrystals were obtained by Sczancoski et al. [35] through a microwave-hydrothermal method at low temperature.

It is known that spherical phosphors with the size of 0.5–3 μm are suitable in application because they increase the screen brightness and improve the resolution due to a lower scattering of evolved light and higher packing density [36]. In addition, the densely packed small spherical particles can prevent phosphors from aging. Nevertheless, if the particle size is too small, luminescence efficiency will be decreased owing to the re-absorption and scattering of light. So far, several research groups have prepared monodisperse $CaWO_4$ microspheres by hydrothermal method but the shape and dispersion of the microspheres were not sufficient [9, 22, 37, 38].

Herein, we therefore report on the morphology-controlled hydrothermal synthesis of quasi-monodisperse AWO_4 (A = Ca, Sr, and Ba) microspheres in the presence of citric acid. The as-synthesized AWO_4 powders were characterized by X-ray powder diffraction (XRD), scanning electron microscopy (SEM), transmission electron microscopy (TEM), and photoluminescence (PL) spectroscopy. The obtained results have demonstrated that the morphologies and particle sizes of the samples can be readily tuned by adjusting the parameters of a hydrothermal process. As a representative of AWO_4, the formation mechanism for $BaWO_4$ microspheres was also studied.

Experimental

All the chemical reagents purchased from Sinopharm Chemical Reagent Beijing Co., Ltd. (China) were of analytical grade and used as received without further purification. Alkaline earth metal orthotungstates, AWO_4 (A = Ca, Sr, and Ba), were synthesized under hydrothermal conditions. Experimental details were as follows: first, 2.5 mmol of respective alkaline earth metal chloride ($CaCl_2{\cdot}2H_2O$, $SrCl_2{\cdot}6H_2O$, or $BaCl_2{\cdot}2H_2O$) was dissolved in 15 mL of deionized water, and then 0.10 g of citric acid ($C_6H_8O_7$) was introduced into the solution. Meanwhile, 2.5 mmol of sodium tungstate (Na_2WO_4) was separately dissolved in 15 mL of deionized water. Then, the sodium tungstate solution was added drop-wise into the alkaline earth metal chloride solution under vigorous stirring, and a white-colored solution was consequently obtained. The pH of the solution was then adjusted to 7 with a 1 M NaOH solution. Finally, the resulting suspension was transferred into a 40 mL Teflon-lined stainless steel autoclave with a filling capacity of 75% and maintained at 180 °C for 8 h. After the hydrothermal system was cooled to room temperature naturally, the precipitates were collected, washed with distilled water several times and dried in air at 60 °C for 4 h.

An X-ray powder diffraction (XRD) analysis was carried out on a D/Max2550 X-ray diffractometer (Rigaku,

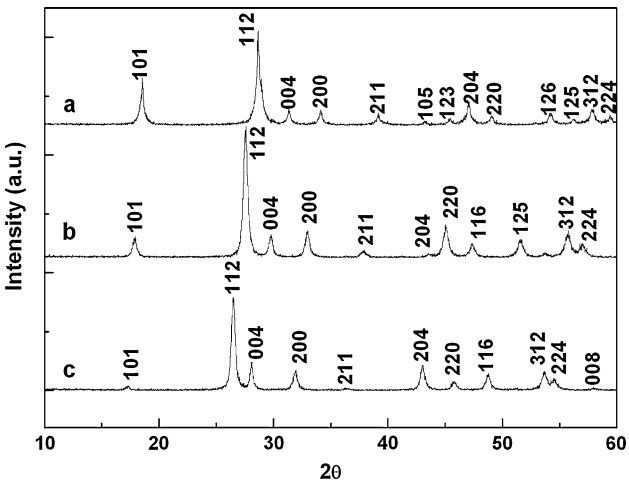

Fig. 1 XRD patterns of AWO_4 powders hydrothermally synthesized at 180 °C for 8 h: $CaWO_4$ (*a*), $SrWO_4$ (*b*), and $BaWO_4$ (*c*)

Japan) with monochromated Cu Kα radiation ($\lambda = 1.5406$ Å) to identify the phase composition and the crystal structure of the as-prepared powders. The samples were scanned at a scanning rate of 4°/min in the 2θ range of 10–60°. The particle sizes and morphologies of the final products were examined using a Quanta 200 scanning electron microscope (FEI, The Netherlands) equipped with an X-ray energy dispersive spectroscopy (EDS), at an acceleration voltage of 15–20 kV. The transmission electron microscopy (TEM) micrographs of the samples were taken with a JEM-2100F transmission electron microscope (JEOL, Japan), operated at an acceleration voltage of 200 kV. The photoluminescence spectra of the samples were measured at room temperature using a LS-55 spectrophotometer (Perkin-Elmer, USA).

Results and discussion

It is known that $CaWO_4$, $SrWO_4$, and $BaWO_4$ having a scheelite-type crystal structure belong to a tetragonal system with the space group of $I41/a(88)$. Figure 1 shows the XRD patterns of AWO_4 powders hydrothermally synthesized at 180 °C for 8 h. As is shown, the hydrothermal treatment of an amorphous precipitate at 180 °C for 8 h resulted in the formation of $CaWO_4$, $SrWO_4$, and $BaWO_4$ phases with good crystallinity. In Fig. 1a, all the diffraction peaks can be readily indexed to the tetragonal $CaWO_4$ phase, according to the JCPDS card no. 72-0257. The calculated lattice constants, $a = 5.252$ Å and $c = 11.388$ Å, are compatible with the previously reported data ($a = 5.243$ Å and $c = 11.376$ Å). All the diffraction peaks in

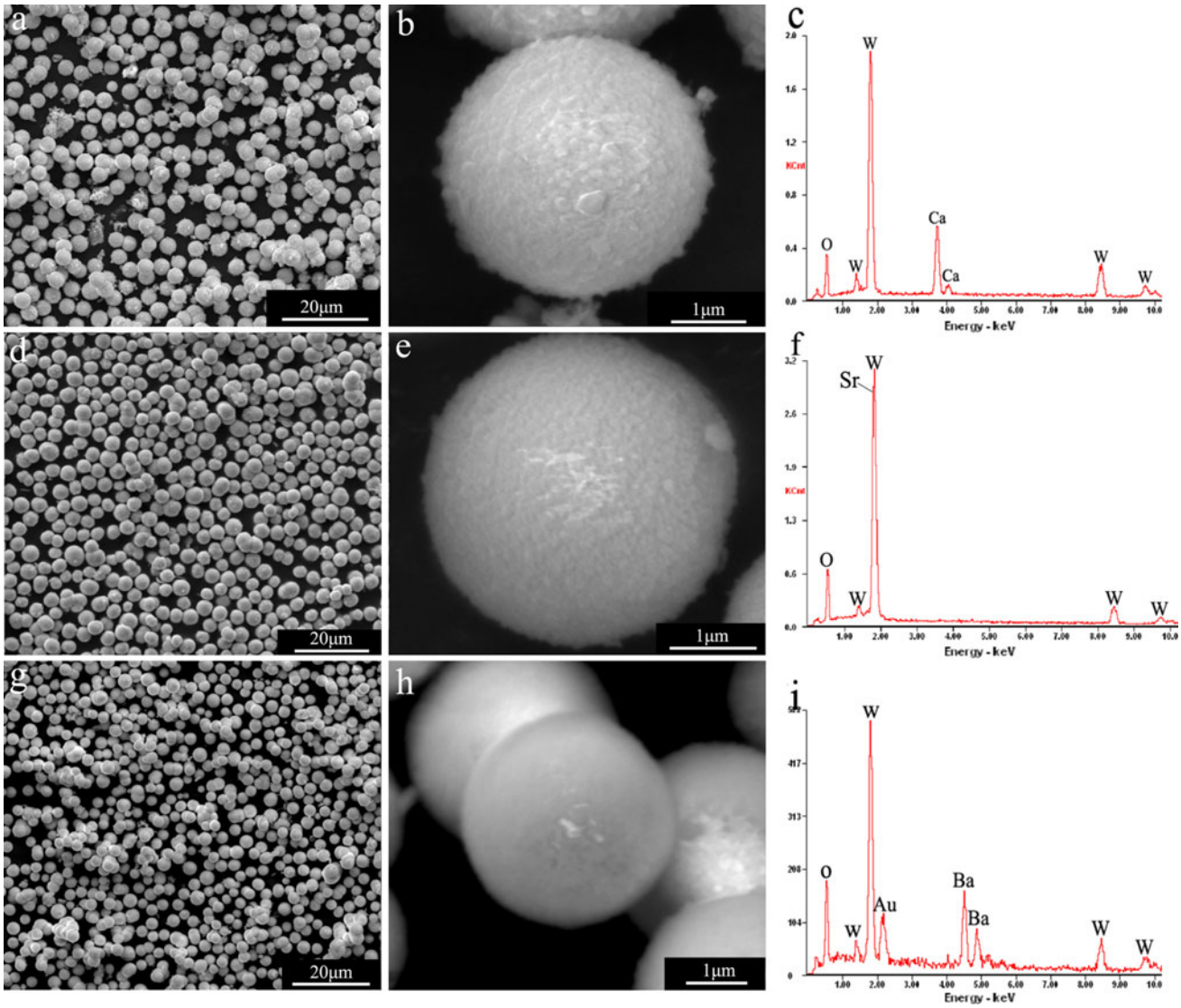

Fig. 2 Low- and high-magnification SEM micrographs and EDS spectra of $CaWO_4$ (*a–c*), $SrWO_4$ (*d–f*), and $BaWO_4$ (*g–i*) powders hydrothermally synthesized at 180 °C for 8 h

Fig. 1b can be well-matched with the tetragonal $SrWO_4$, according to the JCPDS card no. 85-0587. The calculated lattice constants, $a = 5.422$ Å and $c = 11.958$ Å, are consistent with the previously reported data ($a = 5.417$ Å and $c = 11.951$ Å). Figure 1c shows the XRD pattern of $BaWO_4$ powders confirming that the structure of the as-synthesized sample is tetragonal (JCPDS card no. 85-0588). The calculated lattice constants, $a = 5.607$ Å and $c = 12.718$ Å, are in good agreement with the previously reported data ($a = 5.613$ Å and $c = 12.720$ Å). No diffraction peaks belonging to the foreign phases could be detected, indicating high purity of the as-synthesized samples. The crystallite sizes of the as-synthesized samples were calculated using Scherrer's formula: $D = 0.9\lambda/\beta\cos\theta$, where D is the average crystallite size, λ is X-ray wavelength (1.5406 Å), and β is the width of the diffraction peak at half maximum for the diffraction angle 2θ. The estimated crystallite sizes of $CaWO_4$, $SrWO_4$, and $BaWO_4$ powders are found to be 55, 35, and 42 nm, respectively.

The size and morphology information of AWO_4 (A = Ca, Sr, and Ba) powders obtained from scanning electron microscopy (SEM) observation are represented in Fig. 2. Figure 2a shows a low magnification SEM micrograph of $CaWO_4$ powders hydrothermally synthesized at 180 °C for 8 h. It indicates the formation of a large quantity of uniform sphere-like particles in micrometer scale. A high magnification SEM micrograph of $CaWO_4$ powders shown in Fig. 2b reveals that each particle is spherical in shape with the diameter of about 3 μm and is composed of a large number of nanocrystallites. An energy dispersive X-ray spectroscopy (EDS) analysis (Fig. 2c) performed on $CaWO_4$ powders shows that the atomic ratio of Ca:W:O is about 1:1.08:4.12, confirming a possible chemical composition of $CaWO_4$. Figure 2d displays a low magnification SEM micrograph of $SrWO_4$ microspheres hydrothermally synthesized at 180 °C for 8 h. It reveals that the as-synthesized $SrWO_4$ powders also consist of large-scale uniform microspheres with the size of about 2–5 μm in diameter. Figure 2e represents a high magnification SEM micrograph of $SrWO_4$ microspheres. As can be seen, each sphere is constituted of a large number of small nanocrystallites making rough surfaces. An energy dispersive X-ray spectroscopy (EDS) analysis (Fig. 2f) performed on an individual $SrWO_4$ microsphere informs that the atomic ratio of Sr:W:O is about 1:1.03:4.07, which is closer to 1:1:4. Figure 2g shows a low magnification SEM micrograph of the as-prepared $BaWO_4$ powders at 180 °C for 8 h. It clearly evidences that the as-synthesized $BaWO_4$ powders comprise a large quantity of uniform spheres in micrometer size. A high magnification SEM micrograph shown in Fig. 2h imparts that these particles are spherical in shape with the diameter about 4 μm and each microparticle is composed of a large number of small nanocrystallites. An energy dispersive X-ray spectroscopy (EDS) analysis performed on a single $BaWO_4$ microsphere, shown in Fig. 2i, proves that the atomic ratio of Ba:W:O is about 1:0.99:4.05, giving a possible composition of $BaWO_4$.

In order to understand the formation and shape evolution of AWO_4 microspheres, only $BaWO_4$ was chosen as a representative for the time-dependent experiments. The growth process of $BaWO_4$ microspheres was thoroughly examined using XRD, SEM and TEM. The XRD pattern in Fig. 3a indicates that the initial precipitate is fully amorphous without hydrothermal treatment at 180 °C. Obviously, $BaWO_4$ phase starts to crystallize negligibly just after the hydrothermal treatment at 180 °C for 0.5 h (Fig. 3b), whereas an amorphous phase is still dominant. As the hydrothermal treatment time was prolonged to 1 h and longer, the crystallinity of the final products increased considerably (Fig. 3c–f). The XRD patterns clearly demonstrate the evolution of $BaWO_4$ phase from an amorphous to a well-crystalline state with increasing the hydrothermal treatment time at 180 °C. The representative SEM and TEM micrographs of the samples prepared at different hydrothermal treatment periods are shown in Fig. 4. In the early stage of hydrothermal treatment (0.5 h), the obtained white product is mainly composed of small nanoparticles in the size of about 50 nm (Fig. 4a, b). When the reaction time was extended to 1 h, parts of these small nanoparticles tend to agglomerate to form a spherical aggregate, as shown in Fig. 4c. When the reaction time was further increased to 2 h, all the small particles were completely converted into uniform microspheres with an average diameter of about 3 μm (Fig. 4d). When the hydrothermal reaction time finally reached 8 h, the sizes of $BaWO_4$ microspheres increased to nearly 4 μm (Fig. 4e).

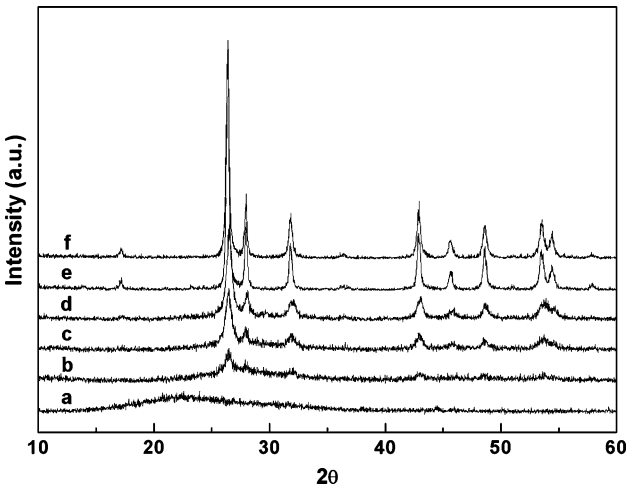

Fig. 3 XRD patterns of $BaWO_4$ powders hydrothermally synthesized at 180 °C for different reaction times: 0 h (*a*), 0.5 h (*b*), 1 h (*c*), 2 h (*d*), 4 h (*e*), and 8 h (*f*)

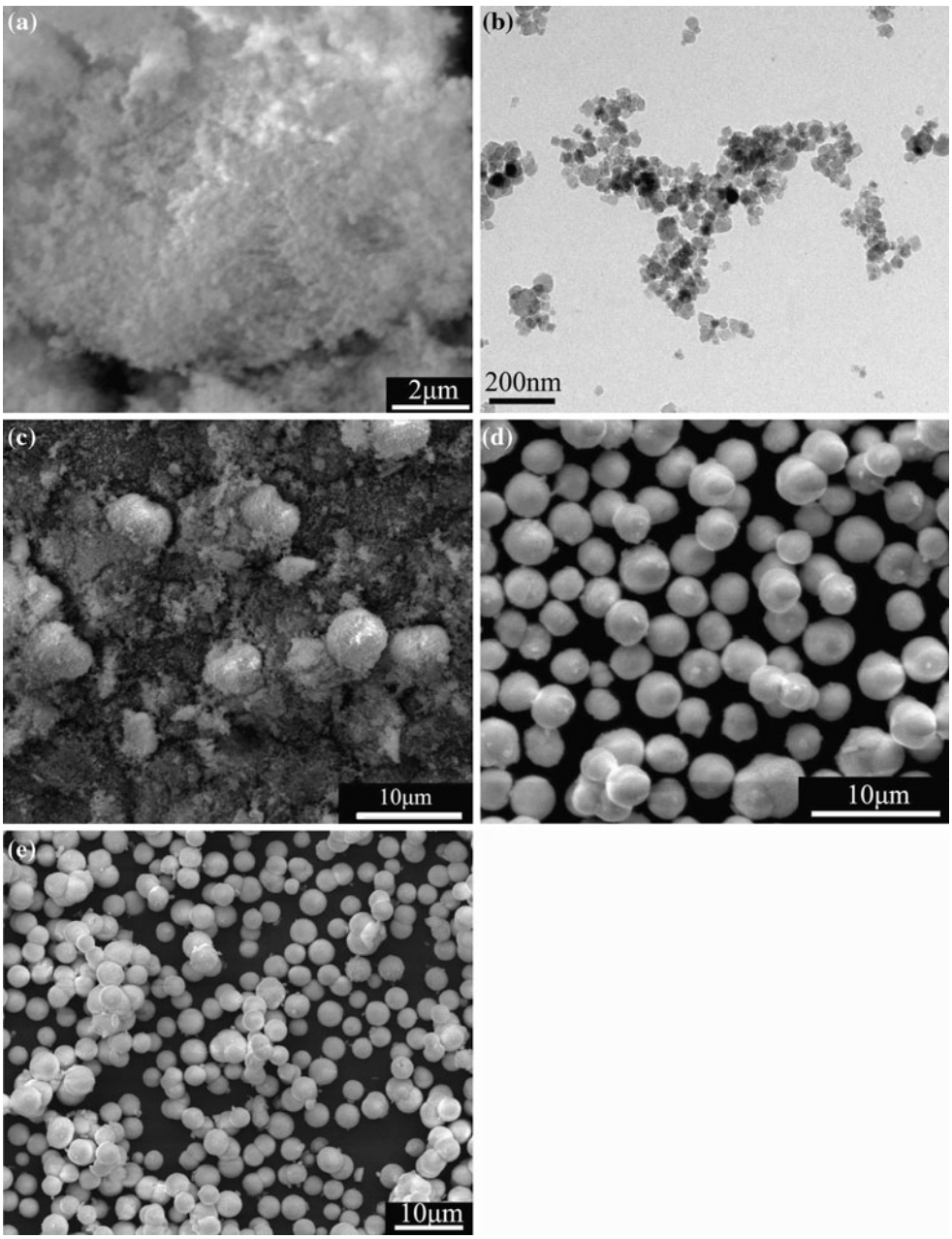

Fig. 4 SEM micrographs of $BaWO_4$ powders hydrothermally synthesized at 180 °C for different reaction times: 0.5 h (**a**–**b**), 1 h (**c**), 2 h (**d**), and 8 h (**e**)

Owing to its relatively weak coordination with metal ions and ability to form certain intermediate complexes at given pH values, citric acid is a suitable complexing agent for the synthesis of inorganic materials with desired morphologies and sizes [39–41]. Nevertheless, the amount of citric acid present in the synthesizing system is important in controlling the sizes and morphologies of inorganic materials. Hereafter, the influence of citric acid amount on the formation of $BaWO_4$ microspheres under hydrothermal conditions at 180 °C for 8 h is also investigated. By adjusting the amount of citric acid in the synthesizing system, $BaWO_4$ with different sizes and morphologies were obtained accordingly, and the corresponding SEM micrographs are illustrated in Fig. 5. In the absence of citric acid in the synthesizing system, large-scale $BaWO_4$ microparticles with the length of about 3–5 μm (Fig. 5a) were obtained; some microparticles present a shuttle-like morphology. Quite similarly, Luo et al. [42] obtained shuttle-like $BaWO_4$ crystals with four prominences in the middle part in the reflux system at 100 °C for 5 min under microwave irradiation in the presence of PVP (0.025 g/mL). By adding 0.03 g of citric acid into the synthesizing system,

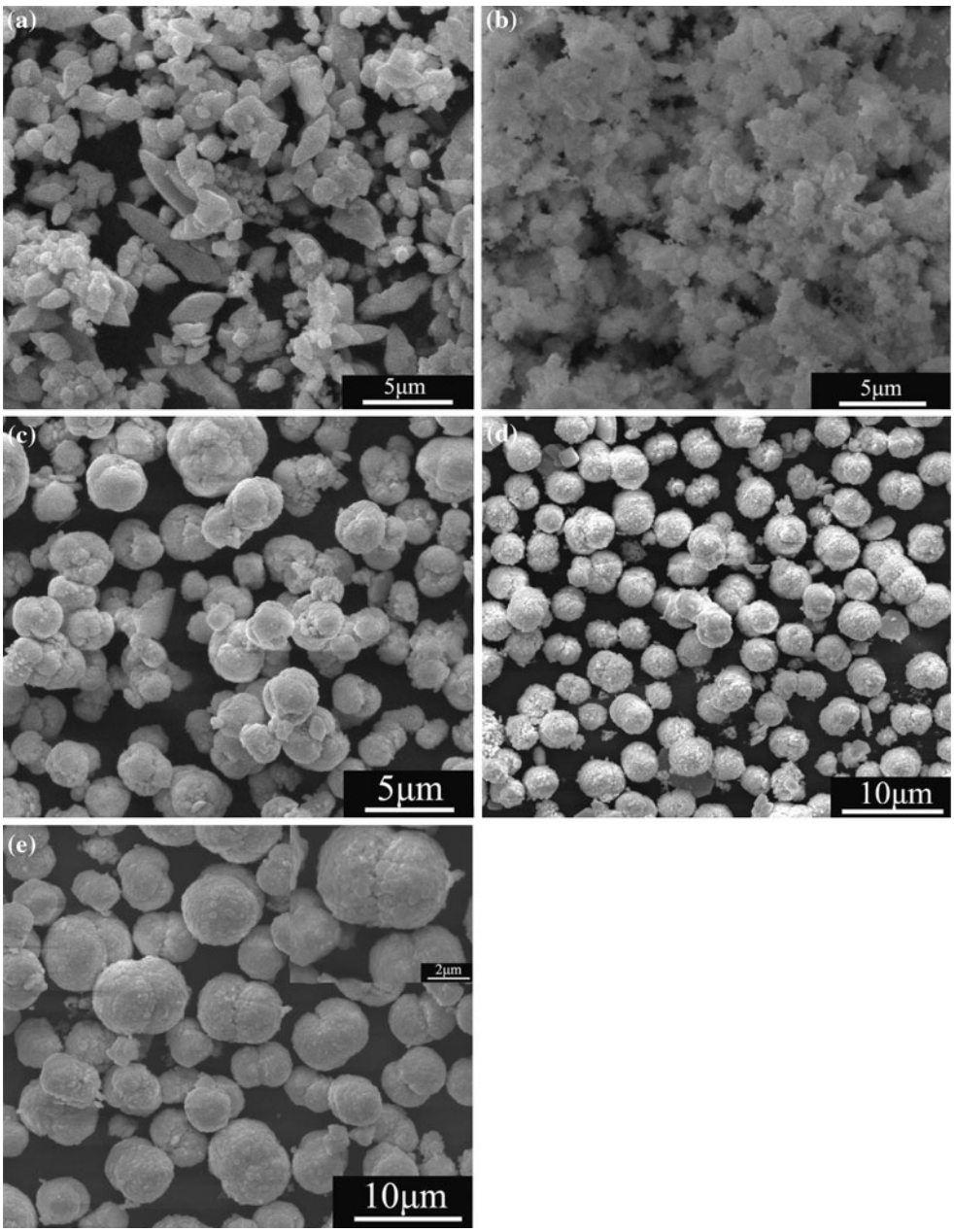

Fig. 5 SEM micrographs of $BaWO_4$ powders hydrothermally synthesized at 180 °C for 8 h with different amounts of citric acid: 0 g (**a**), 0.03 g (**b**), 0.07 g (**c**), 0.15 g (**d**), and 0.20 g (**e**)

$BaWO_4$ nanoparticles were formed (Fig. 5b). Further increase in the amount of citric acid to 0.07 g in the synthesizing system led to the formation of $BaWO_4$ microspheres with the diameter of 2–5 μm (Fig. 5c). In the synthesizing system containing 0.15 g of citric acid, some $BaWO_4$ microspheres possess a peach-like morphology with a clear notch in the middle, as shown in Fig. 5d. With the maximum amount of citric acid (0.20 g) in the system, large-scale complete peach-like $BaWO_4$ microstructures having a height of about 5–8 μm and a width of about 3–5 μm were obtained. It is evident that the amount of citric acid in the synthesizing system plays a governing role in the formation of quasi-monodisperse $BaWO_4$ microspheres.

Based on the obtained results, a possible growth mechanism for quasi-monodisperse AWO_4 (A = Ca, Sr, and Ba) microspheres can be presented as follows. This mechanism can simply be considered as a typical Ostwald ripening process that depicts continuous processes of crystallization/dissolution/recrystallization and morphological transformation of AWO_4 microstructures. In the formation process of AWO_4 microspheres, the hydrothermal treatment time was a crucial factor in controlling the

size and morphology of the final products. First, when ACl_2 (A = Ca, Sr, and Ba) and $C_6H_8O_7$ were mixed together in the solution, an A-($C_6H_5O_7$) complex formed and precipitated, and then the sodium tungstate solution was introduced into the A-($C_6H_5O_7$) complex-containing solution under vigorous stirring. Finally, amorphous AWO_4 precipitates were formed by competing for A^{2+} and $C_6H_5O_7^{2-}$ because AWO_4 is more stable than the A-($C_6H_5O_7$) complex. Some of the $C_6H_5O_7^{2-}$ molecules would also cover the amorphous particles owing to the existent complexing effect between A^{2+} and $C_6H_5O_7^{2-}$ [14]. When the amorphous precursor was hydrothermally treated at 180 °C for 0.5 h, primary nanocrystals with the diameter of 50 nm started to precipitate. With increasing hydrothermal treatment time, the van der Waals interactions between organic molecules took place on the adjacent primary nanocrystals which further promoted the assembly of those primary nanocrystals to form a sphere-like aggregate. Further increase in the hydrothermal treatment time intensively facilitated the growth of AWO_4 microspheres. Meanwhile, some of AWO_4 microspheres dissolved and reprecipitated to form spherical microstructures with relatively smooth surfaces. By the minimization of Gibbs free energy, a ripening process reoccurred until the diameters of the microspheres became relatively uniform.

The room temperature photoluminescence properties of AWO_4 (A = Ca, Sr, and Ba) microspheres were also investigated using an excitation wavelength of 350 nm. Figure 6a–c shows the PL emission spectra of $CaWO_4$, $SrWO_4$, and $BaWO_4$ microspheres hydrothermally synthesized at 180 °C for 8 h, respectively. As can be observed, all three emission spectra exhibit a broad luminescence in the blue spectral range with slightly different intensities. For a comparison, the PL spectrum of the $BaWO_4$ nanocrystallites hydrothermally synthesized at 180 °C for 1 h was also measured and is included in Fig. 6d. Probably, due to the size and crystallinity, this sample shows the lowest intensity in the PL spectra. The different intensities may be resulted from the different sizes and surface properties of quasi-monodisperse AWO_4 microspheres. Similar behavior was noticed in the collective emission spectra of $Ba_{1-x}Sr_xWO_4$ nanorods [18]. The positions of the emission peaks are not considerably altered, implying that the energy band gap relating to the blue emission is not highly affected by the variation in chemical composition of AWO_4 (A = Ca, Sr, and Ba). As mentioned above, the dominant blue emission band of the metal orthotungstates is attributed to the charge-transfer transitions within the $[WO_4^{2-}]$ group between the last fully occupied t_2 orbital and the first empty e orbital [43]. That is, an excitation from the ground state ($^1A_1$) of $[WO_4^{2-}]$ gives rise to four excited states, i.e., $^1T_2$, $^1T_1$, $^3T_2$, and $^3T_1$, from which only the transition between $^1A_1$ and $^1T_2$ is

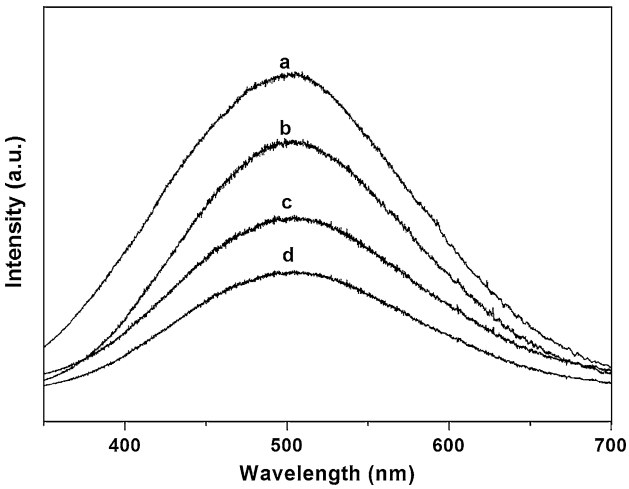

Fig. 6 Room temperature photoluminescence spectra of $CaWO_4$ (*a*), $SrWO_4$ (*b*), and $BaWO_4$ (*c*) powders hydrothermally synthesized at 180 °C for 8 h and $BaWO_4$ nanocrystals (*d*) hydrothermally synthesized at 180 °C for 1 h

electric dipole [44]. During the excitation process at room temperature, the electrons situated at lower intermediary energy levels (oxygen 2p states) absorb the photon energies ($h\nu$) arising from different wavelengths (350 nm ~ 3.54 eV and 488 nm ~ 2.54 eV). As a consequence of this phenomenon, the energetic electrons are promoted to higher intermediary energy levels (tungsten 5d states) located near the conduction band. When the electrons fall back to lower energy states again via radioactive return processes, the energies arising from this electronic transition are converted in photons ($h\nu$). In this case, the several photons ($h\nu$) originated by the participation of different energy states during the electronic transitions are responsible for the broad PL spectra [45].

Conclusions

In summary, quasi-monodisperse AWO_4 (A = Ca, Sr, and Ba) microspheres were successfully fabricated by hydrothermal method at 180 °C for 8 h in the presence of citric acid. The XRD results revealed that AWO_4 powders presenting a scheelite-type tetragonal crystal structure could be hydrothermally synthesized at 180 °C for 8 h without the formation of secondary phases. The SEM and TEM observations confirmed the formation of quasi-monodisperse AWO_4 microspheres under the current hydrothermal conditions. The growth process of $BaWO_4$ microspheres was studied at different hydrothermal reaction times, and a typical Ostwald ripening was considered to be a possible formation mechanism. The effect of citric acid amount present in the synthesizing system was also studied and

found that 0.07 g of citric acid was a favorable amount for the formation of quasi-monodisperse $BaWO_4$ microspheres. The positions of the PL emission peaks were not considerably altered, implying that the energy band gap relating to the blue emission was not greatly affected by the variation in chemical composition of AWO_4 (A = Ca, Sr, and Ba). The obtained quasi-monodisperse AWO_4 microspheres will be potential candidate for a broad range of technological applications, as phosphors, luminescent materials, photocatalysts, etc.

References

1. Sczancoski JC, Bomio MDR, Cavalcante LS, Joya MR, Pizani PS, Varela JA, Longo E, Li MS, Andrés JA (2009) J Phys Chem C 113:5812
2. Marques VS, Cavalcante LS, Sczancoski JC, Alcântara AFP, Orlandi MO, Moraes E, Longo E, Varela JA, Li MS, Santos MRMC (2010) Cryst Growth Des 10:4752
3. Yin Y, Gao Y, Sun Y, Zhou B, Ma L, Wu X, Zhang X (2010) Mater Lett 64:602
4. Cushing BL, Kolesnichenko VL, O'Connor CJ (2004) Chem Rev 104:3893
5. Burda C, Chen X, Narayanan R, El-Sayed MA (2005) Chem Rev 105:1025
6. Chen S-J, Li J, Chen X-T, Hong J-M, Xue Z, You X-Z (2003) J Cryst Growth 253:361
7. Shi H, Qi L, Ma J, Cheng H (2003) J Am Chem Soc 125:3450
8. Liao H-W, Wang Y-F, Liu X-M, Li Y-D, Qian Y-T (2000) Chem Mater 12:2819
9. Zhang Q, Yao W-T, Chen X, Zhu L, Fu Y, Zhang G, Sheng L, Yu S-H (2007) Cryst Growth Des 7:1423
10. Treadaway MJ, Powell RC (1975) Phys Rev B 11:862
11. Li L, Su Y, Li G (2007) Appl Phys Lett 90:054105
12. Gürman E, Daniels E, King JS (1971) J Chem Phys 55:1093
13. Zhuang H, Yue Z, Meng S, Zhao F, Li L (2008) J Am Ceram Soc 91:3738
14. Shan Z, Wang Y, Ding H, Huang F (2009) J Mol Catal A 302:54
15. Cavalcante LS, Sczancoski JC, Lima LF Jr, Espinosa JWM, Pizani PS, Varela JA, Longo E (2009) Cryst Growth Des 9:1002
16. Cavalli E, Boutinaud P, Mahiou R, Bettinelli M, Dorenbos P (2010) Inorg Chem 49:4916
17. Liao J, Qiu B, Wen H-R, Li Y, Hong R, You H (2011) J Mater Sci 46:1184. doi:10.1007/s10853-010-4891-8
18. Cho W-S, Yoshimura M (1997) J Am Ceram Soc 80:2199
19. Zhang F, Sfeir MY, Misewich JA, Wong SS (2008) Chem Mater 20:5500
20. He J, Han M, Shen X, Xu Z (2008) J Cryst Growth 310:4581
21. Shi H, Qi L, Ma J, Wu N (2005) Adv Funct Mater 15:442
22. Liao J, Qiu B, Wen H, Chen J, You W, Liu L (2009) J Alloys Compd 487:758
23. Wang W-S, Zhen L, Xu C-Y, Yang L, Shao W-Z (2008) J Phys Chem C 112:19390
24. Xie B, Wu Y, Jiang Y, Li F, Wu J, Yuan S, Yu W, Qian Y (2002) J Cryst Growth 235:283
25. Jiang X, Ma J, Yao Y, Sun Y, Liu Z, Ren Y, Liu J, Lin B (2009) Ceram Int 35:3525
26. Thongtem T, Phuruangrat A, Thongtem S (2008) Appl Surf Sci 254:7581
27. Dong F-Q, Wu Q-S, Ding Y-P (2009) J Alloys Compd 476:571
28. Cavalcante LS, Sczancoski JC, Espinosa JWM, Varela JA, Pizani PS, Longo E (2009) J Alloys Compd 474:195
29. Luo Z, Li H, Xia J, Zhu W, Guo J, Zhang B (2007) Mater Lett 61:1845
30. Su Y, Li G, Xue Y, Li L (2007) J Phys Chem C 111:6684
31. Chen D, Shen G, Tang K, Zheng H, Qian Y (2003) Mater Res Bull 38:1783
32. Sun L, Cao M, Wang Y, Sun G, Hu C (2006) J Cryst Growth 289:231
33. Liu Y, Chu Y (2005) Mater Chem Phys 92:59
34. Afanasiev P (2007) Mater Lett 61:4622
35. Sczancoski JC, Cavalcante LS, Joya MR, Espinosa JWM, Pizani PS, Varela JA, Longo E (2009) J Colloid Interface Sci 330:227
36. Wang J, Xu Y, Hojamberdiev M (2009) J Alloys Compd 481:896
37. Wang Z, Wang Y, Li Y, Liu B (2010) J Electrochem Soc 157:J125
38. Siqueira KPF, Moreira RL, Valadares M, Dias A (2010) J Mater Sci 45:6083. doi:10.1007/s10853-010-4694-y
39. Zhang H, Yang D, Li S, Ma X, Ji Y, Xu J, Que D (2005) Mater Lett 59:1696
40. Wang W–W (2008) Mater Res Bull 43:2055
41. Yang Z, Liu Q-H, Yang L (2007) Mater Res Bull 42:221
42. Luo Z, Li H, Xia J, Zhu W, Guo J, Zhang B (2007) J Cryst Growth 300:523
43. Grasser R, Scharmann A (1976) J Lumin 12–13:473
44. Grasser R, Scharmann A, Strack K-R (1982) J Lumin 27:263
45. Sczancoski JC, Cavalcante LS, Marana NL, da Silva RO, Tranquilin RL, Joya MR, Pizani PS, Varela JA, Sambrano JR, Siu Li M, Longo E, Andrés J (2010) Curr Appl Phys 10:614